Chapter 1

Results and Discussion

1.1 Validation of P and Q Matrices

Validation of the generated P and Q matrices was done by comparing the energies profiles calculated from them with the copper energy profiles expected from the parameters defined in Bulatov *et al.*'s code. Results from this comparison are shown in Figures 1.1 to 1.3. The calculated energies match exactly the predicted values for all but a few points. Each data set mismatches the expected energy at 1°, and this also occurs at the opposite end for tilt boundaries.

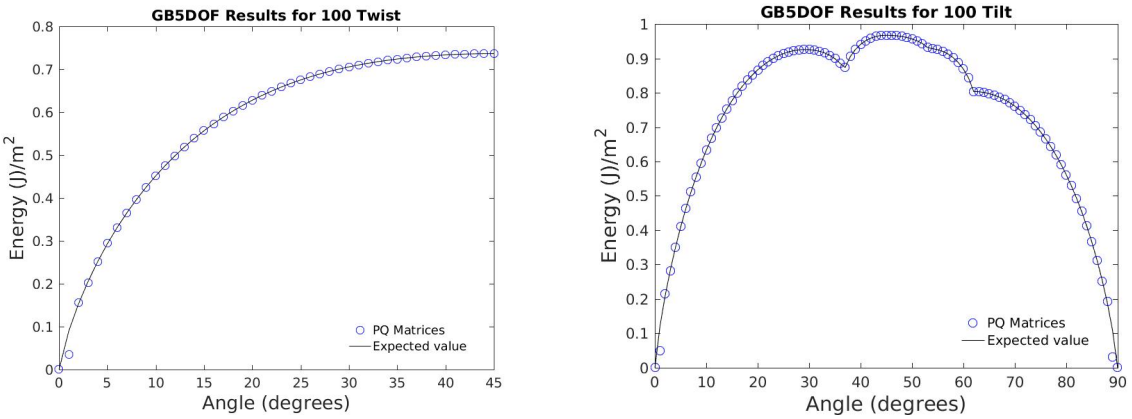

(a) (b)

Figure 1.1: The ⟨100⟩ twist (a) and tilt (b) results for the P and Q matrices as compared to Bulatov *et al.*'s energy profiles. With the exception of the data points at 1° in both (a) and (b) and 89° in (b), the energies calculated from the matrices matches the expected curves exactly.

1.2 Fitting Results

Comparisons for the 1D results from Harbison[1] and this work are presented in Figures 1.4 to 1.6. The results show a general decrease in the GB energies, allowing trends in the different

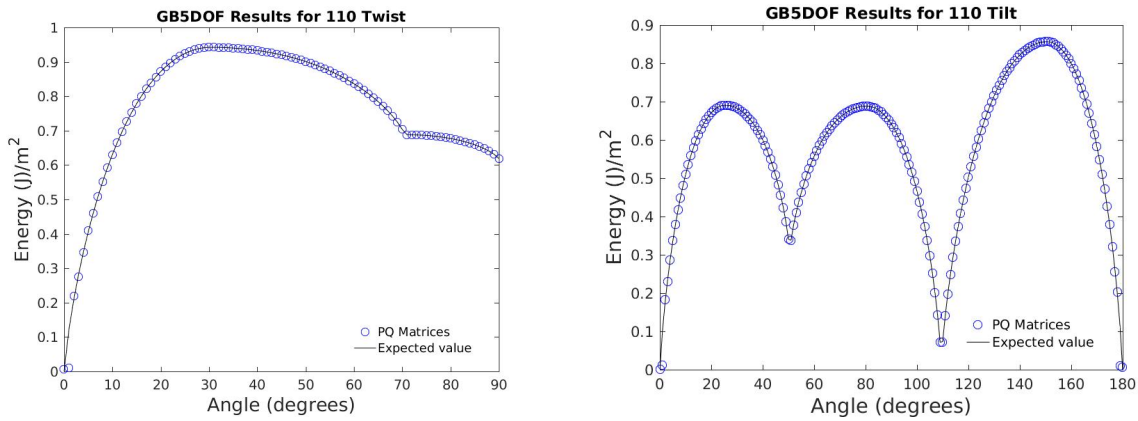

(a) (b)

Figure 1.2: The ⟨110⟩ twist (a) and tilt (b) results for the P and Q matrices as compared to Bulatov *et al.*'s energy profiles. With the exception of the data points at 1° in both (a) and (b) and 179° in (b), the energies calculated from the matrices matches the expected curves exactly.

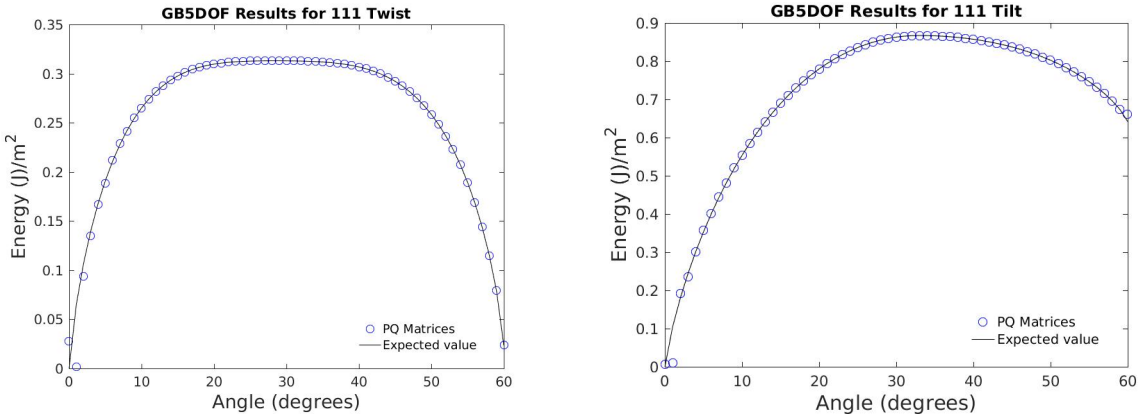

(a) (b)

Figure 1.3: The ⟨111⟩ twist (a) and tilt (b) results for the P and Q matrices as compared to Bulatov *et al.*'s energy profiles. With the exception of the data points at 1° in both (a) and (b) and 60° in (b), the energies calculated from the matrices matches the expected curves exactly.

subsets to emerge. These trends allow for an all around better fit, but there are still some unexpected results present. The parameters that were calculated from the fitting procedure are shown in Table 1.2.

Initial MD recalculations of the ⟨100⟩ symmetric tilt GB energies using the 800 K anneal (Figure 1.4b) showed a deep cusp around 28° which was unexpected. An analysis of the MD simulation results for this misorientation revealed that, in this case, the two crystals had realigned during the simulation due to abnormally high pressures. This caused the misorientation angle to change. This realignment caused the GB energy to be much lower than expected. Comparison with the simulation result used by Harbison revealed that the crystal

structure from his simulation did not realign. While Harbison's data was not calculated with the anneal and thus may not represent a global minimum, the data point follows the trend set by the surrounding data, justifying the use of his result.

Of the symmetric tilt GB energy sets, the ⟨110⟩ set has the most improvement. All three sets showed a general decrease in the energy, giving us confidence that we have achieved a better fit that more accurately describes GB energies in UO_2. However, each of these sets provides more opportunity for research. The ⟨100⟩ set needs more work done for data points after around 50°. The scatter associated with those points seems to be higher, and the possibility of a slight cusp presents itself around 68°. It is unknown what behaviors are expected there though because there are so few data points in that region, so additional data would be beneficial. The ⟨110⟩ set as mentioned shows the most improvement, but there are some low points in the second and third "humps" that do not follow the trend, indicating further possibility for cusps. The first part of the function (the first hump) needs additional data to determine the possibility of a cusp between 40° and 50°. The fitted curve to the ⟨111⟩ set now has an upward trend that is unexpected. The scatter associated with these data points is also relatively high, leading to the possibility of a completely different set of functions to define this subset.

The twist GB energy sets vary in their success. The ⟨100⟩ set shows very little difference between Harbison's[1] work and this work. There is a slight positive concavity at the end of the fitting for this subset, and this is unexpected, indicating the possibility of a cusp. This cusp may occur around 30°. The ⟨110⟩ set has a definite decrease in the overall energies, creating a plateau profile. An additional cusp around 40° is being considered. The ⟨111⟩ set has the least improvement. From the work done by Bulatov *et al.*[2] this work expected to see a plateau as demonstrated by Harbison's[1] fitting. Instead, the fitting produced a curved energy profile, indicating the potential for at least one cusp. A possible location of this cusp is around 35°. Preliminary work has been done with changing the number of parameters in an effort to maximize the quality of the fit with a minimal number of parameters. Figure 1.10 compares the current fitting to the tentative new fitting for three of the six 1D subsets. These modified fits in general seem to fit better at the cost of additional parameters, with a smaller χ^2_{red} value. Still more parameters may be needed to accommodate additional cusps however.

Figures 1.7 to 1.9 show the comparison between the values calculated from the P and Q matrices and the expected values from the MD calculations. There is a scaling issue that has not been solved with the ⟨100⟩ tilt subset. Overall, the results from the P and Q matrices match the fitted values, with a few anomalies that need to be addressed.

1.3 Reduced Chi-square Results

The χ^2_{red} values are much smaller than one for every data set regardless of the method used to calculate the statistic, with the exception of the ⟨100⟩ symmetric tilt subset using the P and Q matrices. This subset has a high χ^2_{red} value due to the scaling issue. Because of the low χ^2_{red} values, the fitted functions are known to overfit the data.[3] Table 1.1 lists the χ^2_{red} values for the 1D subsets using the two different methods for calculation. Equation (1.1) shows the equation used to calculate the χ^2_{red} value:

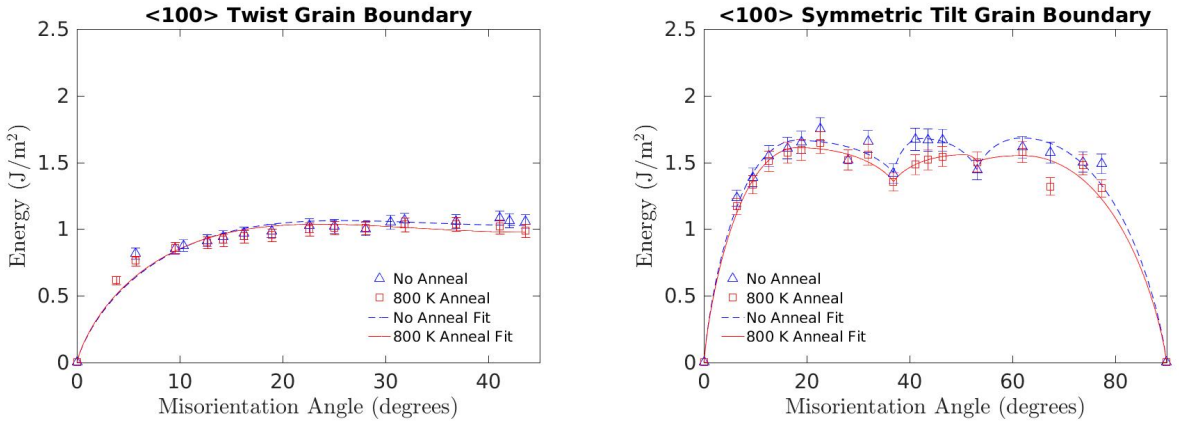

Figure 1.4: The ⟨100⟩ twist (a) and tilt (b) results. In general the re-calculated energies are lower, with significant differences around 40° to 50° in the tilt subset. The positive concavity in the twist subset around 40° is unexpected, and may indicate the presence of a missing cusp. There is a possible cusp around 30° in the twist subset, and around 68° in the tilt subset.

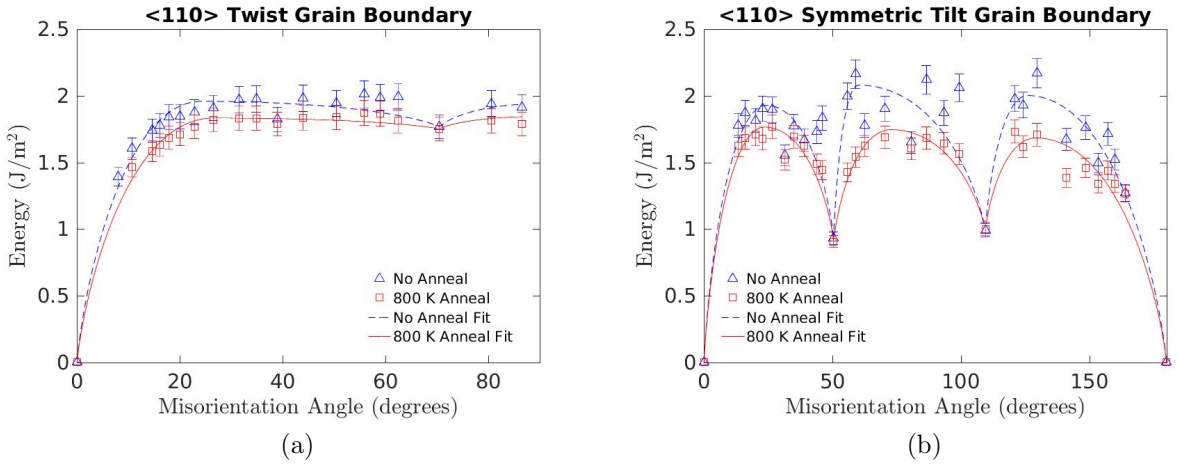

Figure 1.5: The ⟨110⟩ twist (a) and tilt (b) results. Significant decreases in energy are found for both subsets. Possible cusp locations are around 40° in the twist subset, and around 40°, 90°, and 140°in the tilt subset.

$$\chi^2_{\text{red}} = \frac{1}{N-n-1} \sum \frac{(\epsilon_{\text{md}} - \epsilon)^2}{e\ \epsilon_{\text{md}}}. \tag{1.1}$$

In this equation, N is the number of observations, n is the number of parameters, ϵ_{md} are the energies from MD, ϵ are the energies from the model, and e is the uncertainty in the MD results.

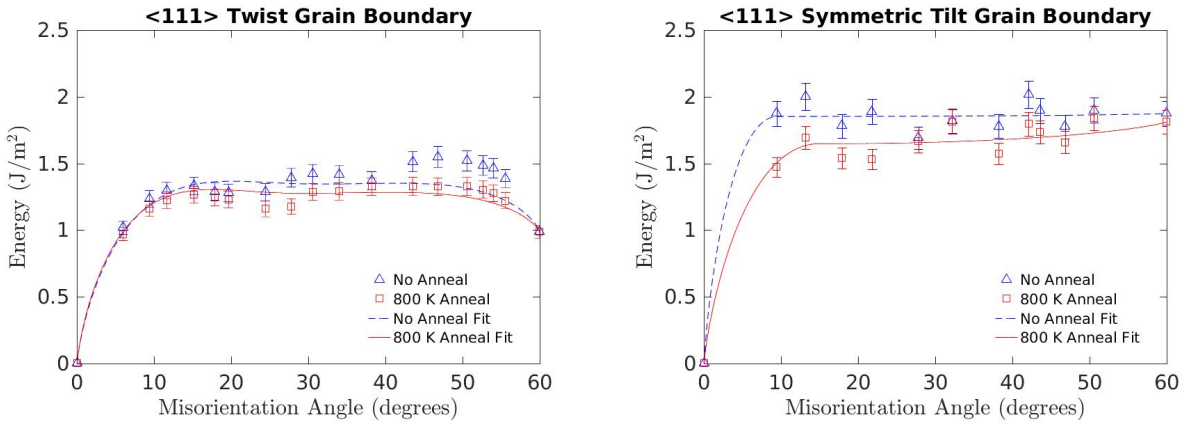

Figure 1.6: The $\langle 111 \rangle$ twist (a) and tilt (b) results. Some energies are found to be lower, but some are also found to be higher. The positive concavity present in these results is unexpected, and could indicate the presence of cusps. A possible location for the twist subset is around 33°. Additional data is needed to determine possible cusp locations for the tilt subset.

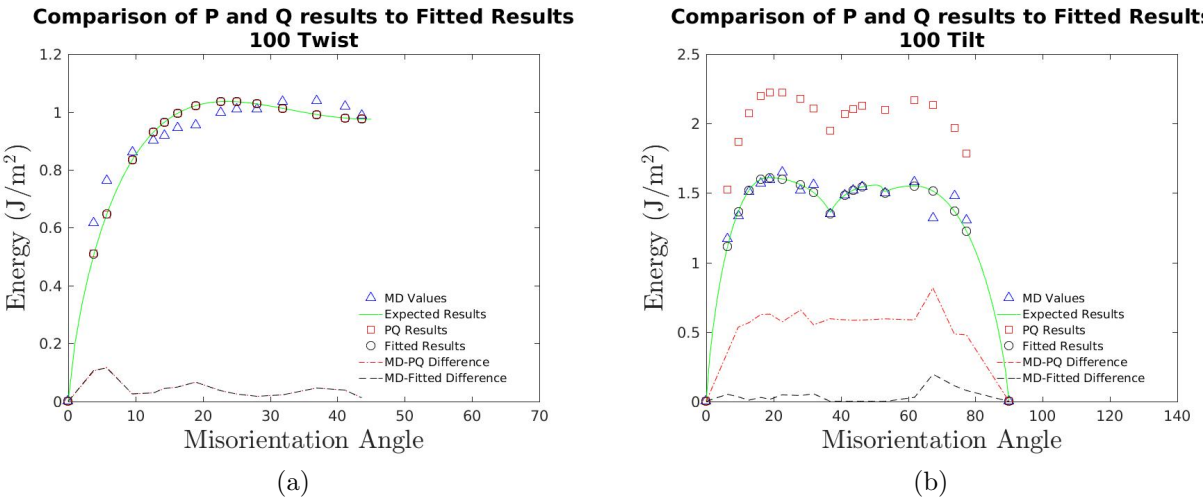

Figure 1.7: A comparison of the expected value of the fitted function with the values calculated using the P and Q matrices for the $\langle 100 \rangle$ 1D subsets. The MD values are shown for reference. (a) PQ results follow exactly the fitted curve. (b) has a scaling issue that has not been fixed. It is uncertain what is causing the scaling issue for this subset.

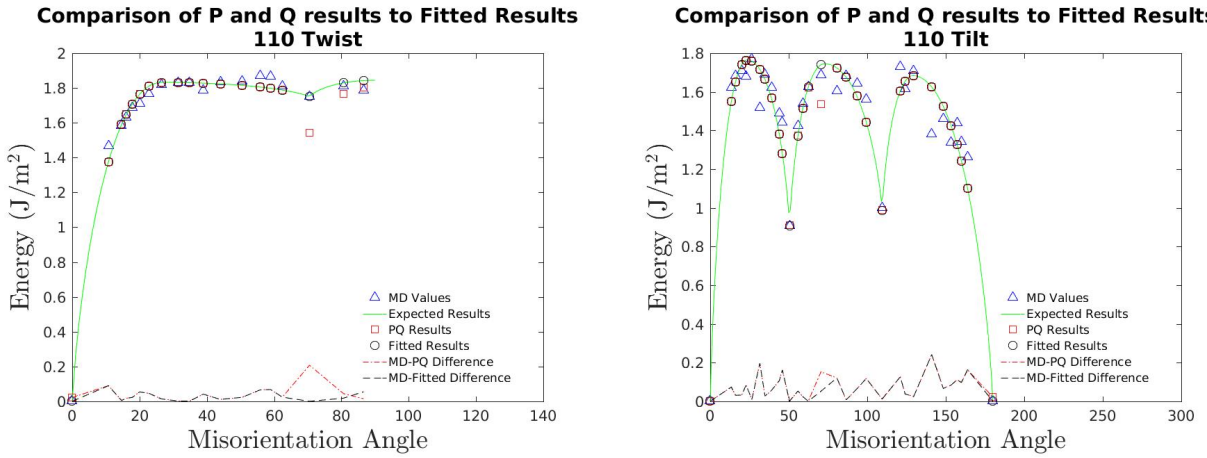

(a) (b)

Figure 1.8: A comparison of the expected value of the fitted function with the values calculated using the P and Q matrices for the ⟨110⟩ 1D subsets. MD values are shown for reference. (a) follows the fitted result until the cusp, at which point some anomalies appear. The results from the PQ matrices dip well below the expected value at the cusp, and never make it back to the original fitted line. (b) has a similar issue on a lesser scale. Only two of the calculated points do not follow the fitted curve. The endpoint is expected to return a zero value, where the PQ matrices calculated a value slightly higher. There is also an unexpected cusp from the PQ matrices in the middle of the second hump. All other data points follow the fitted curve exactly.

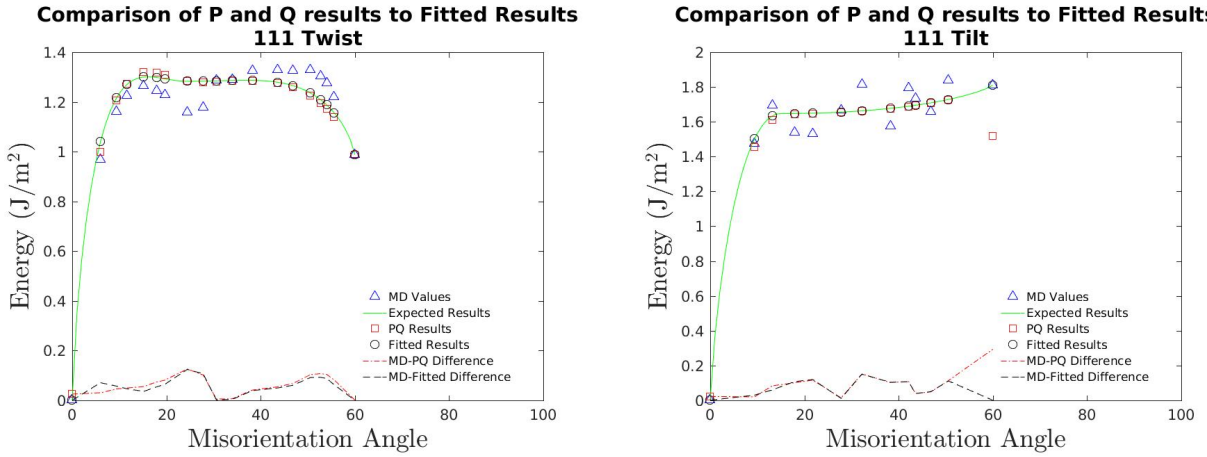

(a) (b)

Figure 1.9: A comparison of the expected value of the fitted function with the values calculated using the P and Q matrices for the ⟨111⟩ 1D subsets. MD values are shown for reference. (a) closely follows the expected fitted values, but has a slight error throughout. (b) follows the expected values exactly in the center of the fitting, but misses slightly for lower angle boundaries, and misses completely at the end.

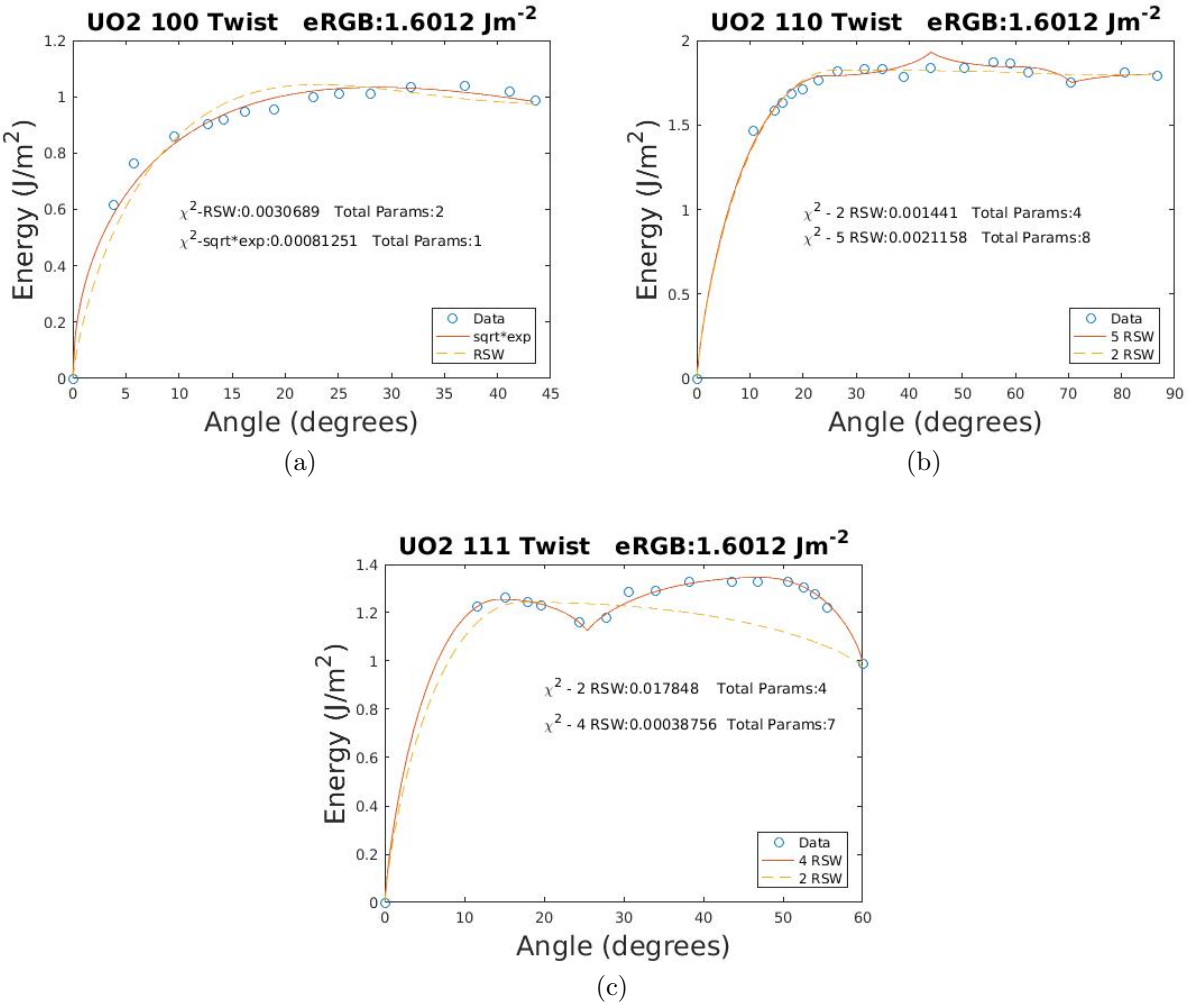

Figure 1.10: An comparison of current fitting functions with a possible change to the functions. Original functions are shown as the dashed lines, with the updated functions shown as the solid lines. MD results are shown for reference. (a) shows a possible change from the RSW functions to a simple square root function multiplied by an exponential decay. There is no theoretical basis behind this change however. (b) attempts to fit to a cusp around 40°. Further work can be done to find a better fit for this subset. (c) shows the most potential improvement. The potential fit increases the total number of parameters by three to fit to the cusp around 28°. A quick glance at the MD values compared to the fit shows a great improvement from the current fit.

Table 1.1: A list of the χ^2_{red} results using two different methods: using the P and Q matrices for the various orientations to test the fit, and comparing the results of the 1D fits to the 1D data. The values for χ^2_{red} are all less than one with the exception of the $\langle 100 \rangle$ symmetric tilt using the P and Q matrices. These values indicate an over-fit to the data.

1D Subset	χ^2_{red} using P and Q matrices		χ^2_{red} comparing the 1D fits	
	No Anneal	800 K Anneal	No Anneal	800 K Anneal
$\langle 100 \rangle$ Twist	0.0953	0.1074	0.0752	0.0722
$\langle 110 \rangle$ Twist	0.1010	0.1874	0.0400	0.0137
$\langle 111 \rangle$ Twist	0.3041	0.1139	0.4966	0.1516
$\langle 100 \rangle$ Tilt	0.1038	8.7702	0.0846	0.0932
$\langle 110 \rangle$ Tilt	4.9799	0.3277	0.5951	0.1762
$\langle 111 \rangle$ Tilt	0.1566	0.7814	0.1315	0.1355
Overall χ^2_{red}	1.7652	1.4893	0.2678	0.1153

Bibliography

[1] T. Harbison, Anisotropic grain boundary energy function for uranium dioxide, B.S. Thesis, Brigham Young University - Idaho, 2015.

[2] V. V. Bulatov, B. W. Reed, and M. Kumar, Acta Mater. **65**, 161 (2014).

[3] P. R. Bevington and D. K. Robison, *Data Reduction and Error Analysis for the Physical Sciences*, McGraw–Hill, New York, NY, 2003.

Table 1.2: This table gives the parameters for UO_2 that generate the energy function.

Array number	Parameter name	Parameter value
1	Energy Scaling Factor (e_{RGB})	1.6012 J/m^2
2	$\langle 100 \rangle$ Max Distance	0.405
3	$\langle 110 \rangle$ Max Distance	0.739
4	$\langle 111 \rangle$ Max Distance	0.352
5	$\langle 100 \rangle$ Weight	50.5
6	$\langle 110 \rangle$ Weight	4.55
7	$\langle 111 \rangle$ Weight	0.08
8	$\langle 100 \rangle$ Tilt/Twist Mix Power Law (1)	0.03325
9	$\langle 100 \rangle$ Tilt/Twist Mix Power Law (2)	0.00053125
10	Maximum $\langle 100 \rangle$ Twist Energy	0.60903
11	$\langle 100 \rangle$ Twist Shape Factor	1.4486
12	$\langle 100 \rangle$ Asymmetric Tilt Interpolation Power	35.8
13	$\langle 100 \rangle$ Symmetric Tilt First Peak Energy	1.0058
14	$\langle 100 \rangle$ Symmetric Tilt First $\Sigma 5$ Energy	0.84456
15	$\langle 100 \rangle$ Symmetric Tilt Second Peak Energy	0.97259
16	$\langle 100 \rangle$ Symmetric Tilt Second $\Sigma 5$ Energy	0.9379
17	$\langle 100 \rangle$ Symmetric Tilt $\Sigma 17$ Energy	0.96881
18	$\langle 100 \rangle$ Symmetric Tilt First Peak Angle	0.31569
19	$\langle 100 \rangle$ Symmetric Tilt Second Peak Angle	0.88538
20	$\langle 110 \rangle$ Tilt/Twist Mix Power Law (1)	3.1573
21	$\langle 110 \rangle$ Tilt/Twist Mix Power Law (2)	1.9784
22	$\langle 110 \rangle$ Twist Peak Angle	0.46145
23	$\langle 110 \rangle$ Twist Peak Energy	1.1444

Continued on next page.

Table 1.2 – *Continued from previous page*

Array number	Parameter name	Parameter value
24	⟨110⟩ Twist Σ3 Energy	1.0931
25	⟨110⟩ Twist 90° Energy	1.152
26	⟨110⟩ Asymmetric Tilt Shape Factor	3.1843
27	⟨110⟩ Symmetric Tilt Third Peak Energy	1.0514
28	⟨110⟩ Symmetric Tilt Σ3 Energy	0.61703
29	⟨110⟩ Symmetric Tilt Second Peak Energy	1.0902
30	⟨110⟩ Symmetric Tilt Σ11 Energy	0.56686
31	⟨110⟩ Symmetric Tilt First Peak Energy	1.1024
32	⟨110⟩ Symmetric Tilt Third Peak Angle	0.88736
33	⟨110⟩ Symmetric Tilt Second Peak Angle	1.8711
34	⟨110⟩ Symmetric Tilt First Peak Angle	2.731
35	⟨111⟩ Tilt-Twist Linear Interpolation	38.201
36	⟨111⟩ Twist Shape Factor	1.2414
37	⟨111⟩ Twist Peak Angle	0.49979
38	⟨111⟩ Twist Peak Energy	0.7971
39	⟨111⟩ Symmetric Tilt Peak Angle	0.25966
40	⟨111⟩ Symmetric Tilt Max Energy	1.0288
41	⟨111⟩ Symmetric Tilt Σ3 Energy	1.1311
42	⟨111⟩ Asymmetric Tilt Symmetry Point Energy	3.7674
43	⟨111⟩ Asymmetric Tilt Scale Factor	0.053417